Article

Properties of 2 mol% Yttria Stabilized Zirconia–Alumina–Cerium Hexaaluminate Composites

Frank Kern

Institute for Manufacturing Technologies of Ceramic Components and Composites (IFKB), University of Stuttgart, Allmandring 7b, D-70569 Stuttgart, Germany; frank.kern@ifkb.uni-stuttgart.de; Tel.: +49-711-685-68233

check for updates

Abstract: Yttria stabilized zirconia (Y-TZP) has become a standard material in a variety of biomedical and mechanical engineering applications due to its high strength and toughness. In order to obtain improved properties in terms of strength, hardness and low temperature degradation resistance second phases, typically alumina are added. In this study an alumina toughened zirconia recipe with 20 vol% alumina in a 2Y-TZP matrix was modified by progressive substitution of alumina by up to 10 vol% cerium hexaaluminate (CA6). Samples were produced by hot pressing. The cerium hexaaluminate was synthesized in situ by reduction of tetravalent ceria and reaction sintering with alumina at 1450 °C. The materials reach attractive 4-point bending strength values of greater than 1170–1390 MPa at a fracture resistance of 6.4–7 MPa$\sqrt{m}$. Vickers hardness is slightly reduced from 1405 HV10 to 1380 HV10 with increasing CA6 fraction. Results show that substitution of alumina by low amounts CA6 does not lead to drastic changes in the mechanical properties. Hardness is slightly reduced while strength reaches a flat maximum at 4 vol% CA6 substitution. The toughness slightly declines with CA6 addition which is caused by reduced transformability of the tetragonal zirconia phase despite a slight coarsening of the matrix observed upon CA6 addition.

Keywords: zirconia; alumina; hexaaluminate; mechanical properties; microstructure

1. Introduction

Since Garvie's paper "ceramic steel" in 1975, zirconia structural ceramics exploiting the effect of transformation toughening have been developed to a state of high maturity and are nowadays used in a multitude of applications such as in dental implants, but also for wear parts or tool inserts in mechanical engineering [1,2]. An excellent overview on the different types of materials is given by Hannink [2]. An in-depth discussion of the transformation toughening effect was published by Kelly [3].

One of the basic issues of zirconia materials over the last decades has been the discrepancy between strength and toughness as outlined by Swain [4]. Ceria stabilized zirconia (Ce-TZP), while having an excellent toughness, has only limited strength and yttria stabilized zirconia (Y-TZP) behaves exactly vice versa [2].

The addition of second phases can be used to tailor the properties of composite ceramics with tetragonal zirconia polycrystal (TZP) matrix. The most popular second phase is alumina which at dopant level (< 1 vol%) drastically increases the ageing stability of Y-TZP [5]. Percentages in the > 10% range lead to high strength [6] and in the best case unchanged toughness for Y-TZP-based composites. For Ce-TZP based composites a suppression of the autocatalytic transformation behavior is observed which leads to higher strength but lower toughness [7]. Ce-TZP/alumina composites with an ultrafine grain microstructure have been proposed for biomedical applications [8,9].

Platelet reinforcement of Ce-TZP has been introduced by Cutler as early as 1991 [7]. It was shown that Ce-TZP/strontium hexaaluminate (SA6) exhibits a higher toughness at identical strength compared to Ce-TZP/alumina composites of the same zirconia/secondary phase volume ratio.

Following Cutler's pioneer work, many studies were published in which Ce-TZP was reinforced with various hexaaluminates of the magnetoplumbite (e.g., SA6) and β-aluminate (LaAl$_{11}$O$_{18}$ = LA6) type [10–12]. Cutler claimed that platelet reinforcement of Y-TZP by SA6 was unsuccessful as the phase does not form [7]. This claim did not hold true [13]. Moreover, the assumption that only SA6 efficiently increases toughness and other hexaaluminates do not is also questionable. It was shown by the author that 12Ce-TZP/30%SA6 materials show more crack deflection than 12Ce-TZP/30%LA6. The overall toughness was, however, almost identical. In the same study it was shown that variation of the hexaaluminates does not only affect crack deflection or crack bridging but also the transformation behavior of the Ce-TZP-matrix, which makes the topic even more complex [14].

In fact up to now only very few systematic studies on platelet reinforced Y-TZP have been published [15]. In an own publication it was shown that the addition of 5 vol% SA6 to an 85% 2.5Y-TZP/15% alumina system only slightly improves the strength and toughness but drastically increases the reliability of as-fired injection molded components [13]. Tsukuma showed that the formation of CeAl$_{11}$O$_{18}$ (CA6) in ceria doped Y-TZP–alumina composites is reversible by changing from reducing to oxidizing conditions and that fracture toughness is not changed while strength is reduced when adding CA6 [16].

From a viewpoint of fracture mechanics, the TZP–hexaaluminate system can be discussed controversially. According to Evans the primary criterion for crack deflection—a positive elastic mismatch—is fulfilled (see equation 1, index R = reinforcement, index M = matrix, values in GPa) so that crack deflection may happen, especially if the platelets are hit by the crack a low angle [17]

$$(E_R - E_M)/(E_R + E_M) = (285-210)/(285 + 210) = 0.15 \qquad (1)$$

However, the hexaaluminate dispersion has a slightly lower coefficient of thermal expansion (CTE) than the matrix, which induces a negative toughness increment [18]. Compared to TZP/alumina the elastic constraint exerted by the hexaaluminate (E ~285 GPa) is lower than for alumina (E ~385 GPa). This should favor phase transformation of the zirconia [19]. A crucial point is probably the strength of the TZP/hexaaluminate interface and the cohesive strength of the hexaaluminate reinforcement which is relevant for the efficiency of crack bridging and stress transfer [17]. Chen assumed that the cohesive strength is not very high compared to other reinforcements such as SiC whiskers [20]. The interface strength is yet unknown, it can however be assumed that the initiation of de-bonding will have a positive correlation to grain size of reinforcements and matrix as the size of residual stress fields scales with grain size [21]. Another consideration is the different R-curve behavior of Y-TZP and Ce-TZP. Transformation zones in Ce-TZP are much larger than in Y-TZP and transformation efficiency is relatively low [2]. Y-TZP shows an extremely steep R-curve with a plateau level at a crack length of a few micrometers while toughness rises steadily in Ce-TZP up to the mm range. Short fiber or platelet reinforcements are a priori more efficient in the rear part of the R-curve, i.e., at higher crack length [22].

Summarizing all these considerations, a spectacular rise in toughness in a Y-TZP of moderate toughness by addition of hexaaluminate platelets is not expected.

In this study a powder produced by detonation synthesis leading to 2Y-TZP ceramics with a toughness of ~10 MPa$\sqrt{m}$ and ~1500 MPa strength was used [23]. This matrix material with a considerable transformability and thereby a high toughness, large transformation zone size and pronounced R-curve behavior was expected to lead to tough composite ceramics with 20 vol.% second phase. It was expected that on this basis a progressive substitution of the second phase alumina by CA6 (while keeping the overall second phase fraction constant) would provide significant evidence to identify and quantify the effects taking place. In situ synthesis of CA6 during hot pressing was applied to guarantee full densification and thereby avoid a skewing of measured values by effects of porosity.

2. Materials and Methods

The powders used for this study are 2Y-TZP (2YSZ, Innovnano, Portugal) produced by detonation synthesis [24], α-alumina (APA0.5, Ceralox, USA) and cerium dioxide (99% purity, Chempur, Germany). For the study five different material compositions were produced with 80 vol% TZP matrix and 20 vol% alumina and CA6 Dispersion. Alumina was successively substituted by CA6 (Compositions: 0% CA6/20% alumina, 2% CA6/18% alumina, 4% CA6/16% alumina, 7% CA6/13% alumina and 10% CA6/10% alumina).

For each batch 200 g of starting powders mixture was dispersed in 300 ml 2-propanol and homogenized by milling in an attrition mill at 500 rpm for 2 h using 600 g of 3Y-TZP milling balls of 2 mm diameter. The milling media were separated by screening and the dispersion was dried at 85 °C overnight. The resulting powder was then screened through a 100 μm mesh. The materials were hot pressed at 1450 °C for 1 h at 50 MPa axial pressure in a boron nitride clad graphite die of 45 mm diameter. Two disks of ~2.5 mm thickness were manufactured in each pressing cycle. Four disks of each composition were pressed. The formation of CA6 was carried out in situ by reducing the ceria and reacting the trivalent ceria with alumina to yield the cerium hexaaluminate phase. In a previous publication it was shown that a sintering temperature of 1450 °C is sufficient to complete the conversion to CA6 [25].

The disks were then pre-ground manually with a 40 μm diamond disk and automatically lapped (15 μm diamond suspension) and polished (15, 6, 3, 1 μm diamond suspension) until a mirror-like finish was obtained on one side, the back side was lapped. Density measurements by buoyancy method, testing of the Young's modulus (impulse excitation technique, IMCE, Belgium) and Vickers hardness measurements (HV10, Bareiss, Germany) were preformed on entire disks. The disks were then cut into bending bars of 4 mm width for 4pt bending strength and fracture toughness. The sides of the bars were lapped with 15 μm diamond suspension to remove cutting-induced defects and the edges were carefully beveled with a 40 μm diamond disk. The bending tests were performed in a 4-point setup with 20 mm outer and 10 mm inner span. Bending strength of 4pt was measured using bars of ~$4 \times 2 \times 25$ mm^3 size and a crosshead speed of 0.5 mm/min (10–15 bars/sample). For the toughness measurements four bars were pre-notched by a Vickers indent (HV10) in the middle of the tensile side (cracks parallel and perpendicular to the sides) and the residual strength was measured in the same 4-point setup at a crosshead speed of 2.5 mm/min. The fracture resistance K_{ISB} was calculated from the residual strength according to Chantikul (ISB = indentation strength in bending) [26]. Resistance to subcritical crack growth was measured by stable indentation crack growth in bending (SIGB). For this test 2 bars were notched with four HV 10 indents placed at a distance of 2 mm along the middle axis of the tensile side. These indented samples were stored for 2 weeks to let the cracks come to a stable extension. Then the growth of the perpendicular indentation-induced cracks was measured at progressive loading steps (crosshead speed 5 mm/min). The starting load was 1/3 of the residual strength of the ISB test. Then the load was increased in 1/10 increments of the residual strength until fracture occurred. After each loading step the crack length was determined by optical microscopy. The final evaluation was carried out according to Dransmann [27]. As proposed in the same publication a geometry factor Ψ of 1.05 was chosen (ideal halfpenny crack Ψ = 1.27) due to the flatter profiles of cracks in Y-TZP materials [27]. The characteristic points in a plot of $\Psi \cdot \sigma \cdot \sqrt{c}$ versus $Pc^{-1.5}$ (Ψ= crack geometry factor, σ = applied bending stress, c = crack length, P = indentation load) are: the ordinate intercept representing K_{IC}, the kink in the curve which is the stress intensity $K_{app,0}$ where the crack starts to grow and the slope between $K_{app,0}$ and K_{IC} which is the residual stress coefficient χ. The difference $K_{IC} - K_{app,0}$ is the threshold toughness K_{I0}, which is relevant for the resistance to subcritical crack growth. $K_{app,0}$ is the R-curve dependent part of the toughness, i.e., the toughness increment contributed by any toughening mechanisms [28]. The phase composition of the composites was determined by X-ray diffraction (XRD) (X'Pert MPD equipped with a X'celerator detector, Panalytical, GB, Bragg Brentano setup, CuKα1, Ge monochromator). The monoclinic/tetragonal ratio was determined by integrating the monoclinic and tetragonal peaks in the 27–32° 2θ range and calculating the monoclinic fraction in polished surfaces

$V_{m,p}$ and in fracture surfaces $V_{m,F}$ according to Toraya [29]. The materials were checked for cubic phase in the 72–76° 2θ range [30], in the same range the tetragonality (c/a-ratio) can be calculated from the location of the (400) and (004) peaks [31]. The presence of cerium aluminates can be identified in the 2θ-range between 32–37 degrees where representative peaks of CA6 (008) at 32.6°, (107) at 34.2° and (114) at 36.3°, as well as of $CeAlO_3$ (110) at 33.7°, are located. It should however be taken into account that trace amounts present in the low CA6 content samples cannot be identified [25].

The size of the transformation zones h can be calculated from XRD data according to Kosmac [32]. Having measured values for Young's modulus E, transformability $V_F = V_{m,F}-V_{m,p}$ and calculated transformation zone size h the transformation toughness increments can be analytically calculated according to McMeeking. It was assumed that the phase transformation is predominantly dilatoric (X = 0.27) [33]. Scanning electron microscope (SEM) images (Hitachi S800, Japan, secondary electrons, acceleration voltage 10 kV) of thermally etched samples (1200 °C/10 min air) were taken to study the microstructure of the different composites.

3. Results

3.1. Microstructure

Figure 1 shows the microstructure of materials of different CA6 contents. The TZP matrix (light grey) consists of equiaxed grains of ~0.5–1 μm size. With progressive substitution of Alumina by CA6 a slight increase in TZP grain size is evident. The alumina (dark grey) is evenly distributed. Compared to the starting powder (d_{50} = 300 nm) a slight coarsening is observed, as alumina grains typically have sizes of 0.3–0.8 μm. Cerium hexaaluminate (grey) forms platelets which are isolated for low CA6 contents and tend to form larger aggregates such as stacks or odd shaped clusters in the case of higher CA6 contents. Isolated plates have a size of 0.4–1 μm width and 2–4 μm length, resulting in an approximate aspect ratio of 4–5. Around the larger CA6 precipitates a depletion of alumina is visible.
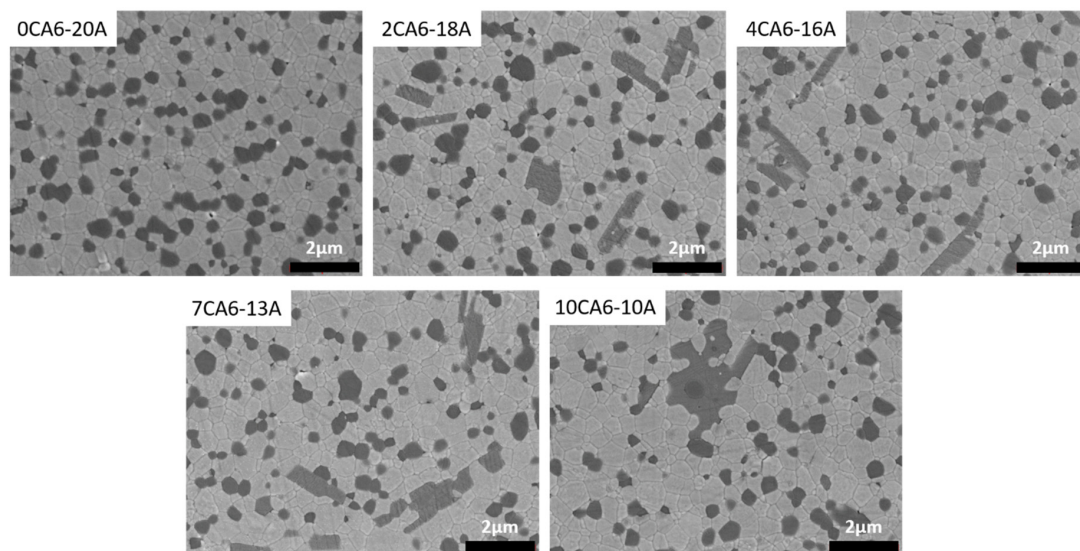
Figure 1. Scanning electron microscope (SEM) images of polished and thermally etched surfaces of different 2Y-TZP/alumina/CA6 composites.

3.2. Mechanical Properties

Figure 2a shows the Young's modulus E and Vickers hardness HV10 of the different composites. The Young's modulus considering the standard deviation of the measurements does not show a statistically relevant trend. Measurement errors in Young's modulus measurements are mainly related to measuring the thickness of the disk (± 2–3 GPa). Based on the rule of mixture we would expect a decline from 245 GPa (20 vol% alumina) to 235 GPa (10 vol% alumina, 10 vol% CA6), this is the range

covered by the measured values. The Vickers hardness HV10 continuously declines from 1407 to 1380 with increasing substitution of alumina by CA6 in line with expectations, here the measurement errors of ± 10 are individual errors incurred in the measurement of the indent size by optical microscopy [20].

(**a**)   (**b**)
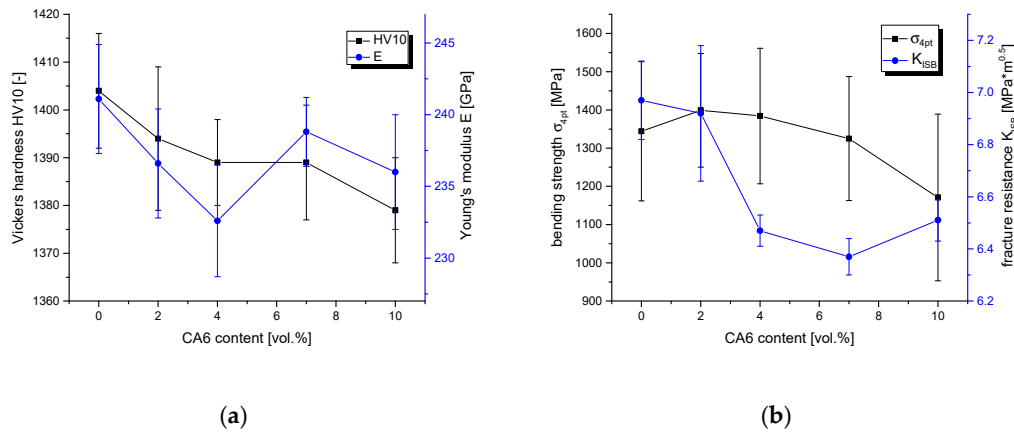
Figure 2. (**a**) Vickers hardness HV10 and Young's modulus E of 2Y-TZP/alumina/CA6 composites depending on CA6 content.   (**b**) Bending strength σ_{4pt} and fracture resistance K_{ISB} of 2Y-TZP/alumina/CA6 composites depending on CA6 content.

The bending strength σ_{4pt} and the fracture resistance K_{ISB} are shown in Figure 2b. All materials show a high bending strength. The trend forms a very flat maximum at 2–4 vol% CA6. Then the strength continuously declines towards higher CA6 fractions. The standard deviations of ± 150–220 MPa are, however, relatively high for all materials. The fracture resistance K_{ISB} is highest for the plain ATZ material. Substitution of alumina by CA6 results in a moderate but distinct loss of toughness, especially between 2–4 vol% CA6 where a decline from ~7 MPa√m to 6.4 MPa√m is observed. At higher CA6 contents the trends levels off and the toughness stays at 6.4–6.5 MPa√m. The standard deviation of toughness measurements are in the range of 0.1–0.2 MPa√m.

The resistance to subcritical crack growth (threshold toughness K_{I0}) was measured by the SIGB method. Figure 3 shows the trends of the toughness increments K_{I0} (threshold) and $K_{app,0}$ (R-curve dependent part). A successive substitution of alumina by CA6 clearly leads to a shift of toughness increments. The threshold increases from 3 MPa√m for ATZ to 4.2 MPa√m for 2Y-TZP-10%CA6/10% alumina. The R-curve dependent increment $K_{app,0}$ drastically reduces from 4 MPa√m to 2.2 MPa√m in the same range. As fatigue resistance may be estimated as $\sigma_F = K_{I0}/K_{IC} \cdot \sigma_{4pt}$ [28], the reduction of the R-curve dependent part of toughness leads to an enhancement of fatigue resistance in the composites from 570 MPa for ATZ to a maximum value of 850 MPa for 2Y-TZP/13% alumina/7%CA6.
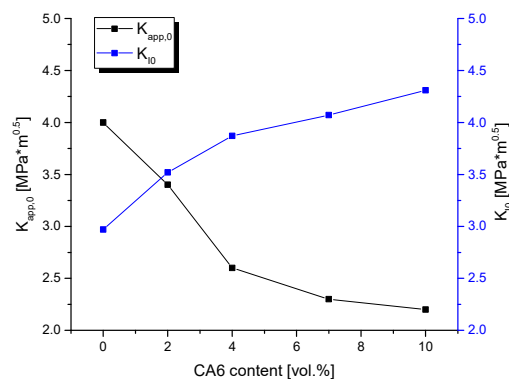
Figure 3.   Toughness increments K_{I0} (threshold) and $K_{app,0}$ (R-curve dependent part) of 2Y-TZP-alumina-CA6 composites depending on CA6 content.

3.3. Phase Composition and Calculation of Transformation Toughness

The monoclinic contents in polished and annealed as well as in fracture surfaces (flat fracture surfaces resulting from ISB tests) were determined by XRD in the 27–33° fingerprint range. Polished and annealed samples are entirely tetragonal except for the plain ATZ, which contains 2.7 vol% monoclinic. Annealing was necessary as the polished samples showed some deformation of the tetragonal (101) peak, indicating machining-induced formation of rhombohedral zirconia [34]. The cubic content was investigated in the 2θ-range between 72–75°. Here only tetragonal (400) and (004) peaks were observed. A peak supposed to be a (400) cubic reflex present in polished samples disappeared after annealing. The tetragonal cell volume and the a and c parameters of the tetragonal phase were determined [30]. Figure 4a shows the transformability $V_F = V_{m,f} - V_{m,p}$. The c/a ratio representing the tetragonality of the zirconia is also plotted for different contents of CA6. From a and c values calculation the unit cell size was calculated (not shown in detail).

(a)   (b)
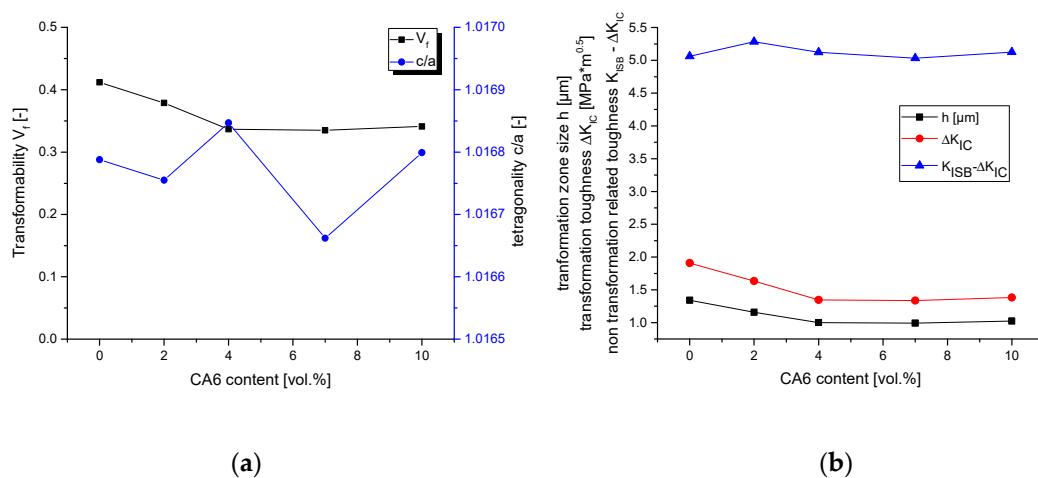
Figure 4. (**a**) Transformability V_f and tetragonality c/a 2Y-TZP/alumina/CA6 composites depending on CA6 content. (**b**) Transformation zone size h, transformation toughness increment $\Delta K_{IC}{}^T$ and non-R-curve related toughness $K_{NR} = K_{ISB} - K_{IC}{}^T$

As shown, the transformability V_f of the tetragonal phase declines with increasing CA6 content. From 4 vol% CA6 upwards a constant value V_f = 35 % is obtained. The c/a ratio changes only very little from 1.01665 to 1.01685. As can be expected from the Y-TZP starting powder this c/a ratio corresponds to a stabilizer content of ~ 2 mol% according to the calibration curve of Scott [30]. The size of the unit cell does not change significantly (only by a factor of $<10^{-4}$). An influence of ceria addition on the tetragonality of the TZP matrix can therefore be neglected.

Based on the phase composition of polished and fractured material it is possible to calculate the size of the transformation zones h and the transformation toughness increments $\Delta K_{IC}{}^T$ for the different compositions [32,33]. Figure 4b shows the calculated values for h and $\Delta K_{IC}{}^T$. By subtracting the value of $\Delta K_{IC}{}^T$ from the measured fracture resistance K_{ISB} the non-transformation related toughness $K_{NT} = K_{ISB} - \Delta K_{IC}{}^T$ can be estimated.

Transformation zone sizes and transformation toughness values as well as fracture resistance show an identical trend. It is shown that the non-transformation related toughness $K_{NT} = K_{ISB} - \Delta K_{IC}{}^T$ is 5.1 ± 0.1 MPa√m for all materials.

In the fingerprint range at 32–35° 2θ only the 107 peak of CA6 at 34.1° was observed (JCPDS 48–0055), no characteristic 110 peak of $CeAlO_3$ (JCPDS 28–0260) was visible at 33.6° (only done for the highest degree of CA6 substitution)

4. Discussion

The initial question for this study was to find out if and to what extent a hexaaluminate platelet reinforcement can increase the strength and toughness of Y-TZP. Putting all collected evidence together, it seems that a platelet reinforcement may lead to a moderate improvement of strength but—this was quite unexpected—also to a reduction of the toughness if alumina is successively replaced by CA6. While it is difficult to give a quantitative explanation for the improved strength, the decline in toughness can be directly correlated to a reduction of the transformability of the matrix.

A closer look at Figure 1 gives some hints that for low fractions of CA6 addition a tri-phasic composite is obtained in which the two dispersions, alumina and CA6, are very homogeneously distributed in the TZP matrix. For higher CA6 contents the hexaaluminates tend to form larger and more irregular aggregates which may act as structural defects. Moreover, at a high fraction of CA6 a significant fraction of the fracture face consists of fractured hexaaluminate, a phase with low cleavage strength [20]. This may explain the lower strength at 10 vol% CA6.

It was shown that increasing the CA6 content leads to a decrease of transformability of the zirconia, which as a consequence leads to decrease of the transformation toughness increment ΔK_{IC}^{T} from 1.9 to 1.4 MPa$\sqrt{m}$. This fact consistently explains the change in fracture resistance.

Some issues are, however, yet unclear. Upon addition of CA6 actually an increase of TZP grain size can be observed, which should boost transformation toughening rather than reducing it.

It might be suggested that adding a lot of ceria would lead to an incorporation of ceria into the TZP lattice, increasing the stabilizer content and reducing the transformability. Therefore, it was checked if the tetragonality of the TZP phase is changed. The change in unit cell size and c/a ratio are however negligible. As shown by Zhang the change of the lattice parameters of 3Y-TZP due to incorporation of large trivalent dopants is very moderate but the c/a ratio reacts very sensitively. While there is no measurable uptake of tri- or tetravalent ceria into the bulk solid solution it may well be that there is some Ce^{3+} (an oversized cation like La^{3+}) uptake in the TZP grain boundaries which is responsible for the moderate decrease in transformability [35].

Some entrapped zirconia grains in the CA6 platelets are an indication that the platelet formation involves a zirconia containing intermediate such as pyrochlore type $Ce_2Zr_2O_7$, as in the case of lanthanum hexaaluminate formation investigated by Miura [10].

$$2\ CeO_2 + CO \rightarrow Ce_2O_3 + CO_2 \tag{2}$$

$$Ce_2O_3 + Al_2O_3 \rightarrow 2CeAlO_3 \tag{3}$$

$$Ce_2O_3 + 2ZrO_2(Y) \rightarrow Ce_2Zr_2O_7(Y) \tag{4}$$

$$Ce_2Zr_2O_7 + Al_2O_3 \rightarrow 2CeAlO_3 + 2\ ZrO_2(Y) \tag{5}$$

$$CeAlO_3 + 5\ Al_2O_3 \rightarrow CeAl_{11}O_{18} \tag{6}$$
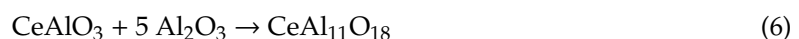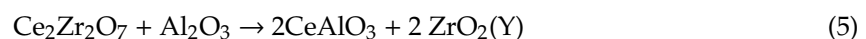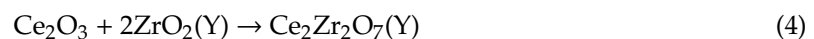
It is yet unclear if the cerium hexaaluminate formation follows the track (2) → (3) → (6) or (2) → (4) → (5) → (6) or both. However, the consolidation cycle by hot pressing was relatively fast and no remaining intermediate phases were detected in the sintered specimen. Even at the highest CA6 content a surplus of 100% alumina is present. Hence, it is likely that the reaction proceeds towards the hexaaluminate (JCPDS 48–0055) and that no or only a small fraction of monoaluminate (JCPDS 28–0260) invisible by XRD remains.

The fact that the change in transformability fully explains the change of toughness and that the non-transformation related toughness K_{NT} stays at a constant value of ~5 MPa$\sqrt{m}$ may lead to two a

priori assumptions. Either K_{NT} is the actual intrinsic toughness of the material and no other process zone-related effects (R-curve behavior) exist or the changes of intrinsic toughness and other R-curve related effects (microcracking, crack deflection, crack bridging) perfectly compensate for each other.

5. Conclusions

The exchange of alumina in alumina toughened zirconia by cerium hexaaluminate does not lead to enhanced strength and toughness. Strength stays on a relatively constant level from 0–7 vol% CA6. Toughness shows a significant decline at CA6 contents above 2 vol%. The reduction of toughness is caused by a reduction of transformability of the tetragonal phase of zirconia.

Still, these materials are of high interest for, e.g., biomedical applications such as dental implants as their fatigue resistance is drastically enhanced compared to plain alumina toughened zirconia (σ_F ~570 MPa) or biomedical grade 3Y-TZP (σ_F ~500–600 MPa). While some damage tolerance for single catastrophic events has to be sacrificed, the far superior fatigue strength (σ_F ~850 MPa at 7% CA6) caused by simultaneous increase of the threshold toughness and a reduction of the R-curve dependent part of toughness would provide high reliability in applications operating under constant or alternating loading conditions.

Conflicts of Interest: The authors declare no conflict of interest.

References

1. Garvie, R.C.; Hannink, R.H.; Pascoe, R.T. Ceramic steel? *Nature* **1975**, *258*, 703–704. [CrossRef]
2. Hannink, R.H.J.; Kelly, P.M.; Muddle, B.C. Transformation Toughening in Zirconia-Containing Ceramics. *J. Am. Ceram. Soc.* **2000**, *83*, 461–487. [CrossRef]
3. Kelly, P.M.; Francis Rose, L.R. The martensitic transformation in ceramics—Its role in transformation toughening. *Prog. Mater. Sci.* **2002**, *47*, 463–557. [CrossRef]
4. Swain, M.V.; Rose, L.R.F. Strength Limitations of Transformation-Toughened Zirconia Alloys. *J. Am. Ceram. Soc.* **1986**, *69*, 511–518. [CrossRef]
5. Ross, I.M.; Rainforth, W.M.; McComb, D.W.; Scott, A.J.; Brydson, R. The role of trace additions of alumina to yttria partially stabilized zirconia (Y-TZP). *Scripta Materialia.* **2001**, *45*, 653–660. [CrossRef]
6. Tsukuma, K.; Ueda, K.; Shimada, K. Strength and Fracture Toughness of Isostatically Hot-Pressed Composites of Al_2O_3 and Y_2O_3-Partially-Stabilized ZrO_2. *J. Am. Ceram. Soc.* **1985**, *68*, C4–C5. [CrossRef]
7. Cutler, R.A.; Mayhew, R.J.; Prettiman, K.M.; Virkar, A. High-Toughness Ce-TZP/Al_2O_3 Ceramics with Improved Hardness and Strength. *J. Am. Ceram. Soc.* **1991**, *74*, 179–186. [CrossRef]
8. Nawa, M.; Nakamoto, S.; Sekino, T.; Niihara, K. Tough and Strong Ce-TZP/Alumina Nanocomposites Doped with Titania. *Ceram. Int.* **1998**, *24*, 497–506. [CrossRef]
9. Benzaid, R.; Chevalier, J.; Saâdaoui, M.; Fantozzi, G.; Nawa, M.; Diaz, L.A.; Torrecillas, R. Fracture toughness, strength and slow crack growth in a ceria stabilized zirconia–alumina nanocomposite for medical applications. *Biomaterials* **2008**, *29*, 3636–3641. [CrossRef]
10. Miura, M.; Hongoh, H.; Yogo, T.; Hirano, S.; Fujii, T. Formation of plate-like lanthanum-13-Aluminate crystal in Ce-TZP matrix. *J. Mat. Sci.* **1994**, *29*, 262–268. [CrossRef]
11. Yamaguchi, T.; Sakamoto, W.; Yogo, T.; Fujii, T.; Hirano, S. In situ formation of Ce-TZP/Ba-Hexaaluminate composites. *J. Ceram. Soc. Jpn.* **1999**, *107*, 814–819. [CrossRef]
12. Tsai, J.F.; Chon, U.; Ramachandran, N.; Shetty, D.K. Transformation Plasticity and Toughening in CeO_2-Partially-Stabilized Zirconia–Alumina (Ce-TZP/Al_2O_3) Composites Doped with MnO. *J. Am. Ceram. Soc.* **1992**, *75*, 1219–1238. [CrossRef]
13. Kern, F.; Gadow, R. Influence of In-Situ Platelet Reinforcement on the Properties of Injection Moulded Alumina-Toughened Zirconia. *J. Ceram. Sci. Technol.* **2011**, *2*, 47–54.

14. Kern, F. A comparison of microstructure and mechanical properties of 12Ce-TZP reinforced with alumina and in situ formed strontium- or lanthanum hexaaluminate precipitates. *J. Eur. Ceram. Soc.* **2014**, *34*, 413–423. [CrossRef]

15. Gottwik, L.; Wippermann, A.; Kuntz, M.; Denkena, B. Effect of strontium hexaaluminate addition on the damage-tolerance of yttria-stabilized zirconia. *Ceram. Int.* **2017**, *43*, 15891–15898. [CrossRef]

16. Tsukuma, K. Conversion from β-$Ce_2O_3 \cdot 11$ Al_2O_3 to α-Al_2O_3 in Tetragonal ZrO_2 Matrix. *J. Am. Ceram. Soc.* **2000**, *83*, 3219–3221. [CrossRef]

17. Evans, A.G.; He, M.Y.; Hutchinson, J.W. Interface Debonding and Fiber Cracking in Brittle Matrix Composites. *J. Am. Ceram. Soc.* **1989**, *72*, 2300–2303. [CrossRef]

18. Schmid, C.; Lucchini, E.; Sbaizero, O.; Maschio, S. The Synthesis of Calcium or Strontium Hexaluminate Added ZTA Composite Ceramics. *J. Eur. Ceram. Soc.* **1999**, *19*, 1741–1746. [CrossRef]

19. Lange, F.F. Transformation toughening—Part 3: Experimental Observations in the ZrO_2-Y_2O_3-System. *J. Mater. Sci.* **1982**, *17*, 240–246. [CrossRef]

20. Chen, P.L.; Chen, I.W. In-Situ Alumina/Aluminate Platelet Composites. *J. Am. Ceram. Soc.* **1992**, *75*, 2610–2612. [CrossRef]

21. Kingery, D.; Bowen, H.K.; Uhlmann, R. *Introduction to Ceramics*; Wiley: New York, NY, USA, 1976; p. 785.

22. Becher, P.F.; Hsueh, C.-H.; Angelini, P.; Tiegs, T.N. Toughening Behavior in Whisker-Reinforced Ceramic Matrix Composites. *J. Am. Ceram. Soc.* **1988**, *71*, 1050–1061. [CrossRef]

23. Kern, F.; Reveron, H.; Chevalier, J.; Gadow, R. Mechanical behaviour of extremely tough TZP bioceramics. *J. Mech. Behav. Biomater.* **2018**, *90*, 395–403. [CrossRef] [PubMed]

24. Calado, J. Ceramic powder production with emulsion detonation synthesis. *CFI/Ber. DKG* **2016**, *93*, E32–E34.

25. Kern, F. Effect of In Situ-Formed Cerium Hexaaluminate Precipitates on Properties of Alumina -24 Vol% Zirconia (1.4Y) Composites. *J. Ceram. Sci. Technol.* **2013**, *4*, 177–186.

26. Chantikul, P.; Anstis, G.R.; Lawn, B.R.; Marshall, D.B. A Critical Evaluation of Indentation Techniques for Measuring Fracture Toughness: II, Strength method. *J. Am. Ceram. Soc.* **1981**, *64*, 539–543. [CrossRef]

27. Dransmann, G.W.; Steinbrech, R.W.; Pajares, A.; Guiberteau, F.; Dominguez-Rodriguez, A.; Heuer, A. Indentation Studies on Y_2O_3-Stabilized ZrO_2: II, Toughness Determination from Stable Growth of Indentation-Induced Cracks. *J. Am. Ceram. Soc.* **1994**, *77*, 1194–1201. [CrossRef]

28. De Aza, A.H.; Chevalier, J.; Fantozzi, G.; Schehl, M.; Torrecillas, R. Slow-Crack-Growth Behavior of Zirconia-Toughened Alumina Ceramics Processed by Different Methods. *J. Am. Ceram. Soc.* **2003**, *86*, 115–120. [CrossRef]

29. Toraya, H.; Yoshimura, M.; Somiya, S. Calibration Curve for Quantitative Analysis of the Monoclinic-Tetragonal ZrO_2 System by X-Ray Diffraction. *J. Am. Ceram. Soc.* **1984**, *67*, C119–C121.

30. Nakayama, S.; Maekawa, S.; Sato, T.; Masuda, Y.; Imai, S.; Sakamoto, M. Mechanical properties of ytterbia stabilized zirconia ceramics (Yb-TZP) fabricated from powders prepared by co-precipitation method. *Ceram. Int.* **2000**, *26*, 207–211. [CrossRef]

31. Scott, H.G. Phase relationships in the zirconia-yttria system. *J. Mater. Sci.* **1975**, *10*, 1527–1535. [CrossRef]

32. Kosmac, T.; Wagner, R.; Claussen, N. X-ray Determination of Transformation Depths in Ceramics Containing Tetragonal ZrO_2. *J. Am. Ceram. Soc.* **1981**, *64*, C72–C73. [CrossRef]

33. McMeeking, R.M.; Evans, A.G. Mechanics of Transformation-Toughening in Brittle Materials. *J. Am. Ceram. Soc.* **1982**, *65*, 242–246. [CrossRef]

34. Kao, H.C.; Ho, F.Y.; Yang, C.C.; Wei, W.J. Surface machining of Fine-grain Y-TZP. *J. Eur. Ceram. Soc.* **2000**, *20*, 2447–2455. [CrossRef]

35. Zhang, F.; Vanmeensel, K.; Inokoshi, M.; Batuk, M.; Hadermann, J.; van Meerbeek, B.; Naert, I.; Vleugels, J. 3Y-TZP ceramics with improved hydrothermal degradation resistance and fracture toughness. *J. Eur. Ceram. Soc.* **2014**, *34*, 2453–2463. [CrossRef]